

# Chapter 12

## Effect of Microstructures on Char Combustion Reactivity



Jingyuan Li, Lele Feng, Yiqun Huang, Yang Zhang, Lyu Junfu,  
and Man Zhang

**Abstract** Reaction of char dominates the combustion of coal in terms of the time scale and heat release, thus study on the reactivity of char is essential. Some researchers found that the coal char combustion reactivity is the function of its microstructure and the devolatilization temperature. However, in the related reported studies, the coal types used in the experiments were limited. Therefore, in this paper series of systematic experiments were conducted with 12 types of coal, including anthracite, bituminous, lean coal and lignite, and the volatile matter content ranges from 5 to 55%. The char samples were prepared in the muffle furnace in ambient atmosphere at 900 °C. The thermogravimetry analyzer (TGA) was employed to evaluate the char combustion reactivity. Moreover, the microstructure of the char was measured by X-Ray Diffraction (XRD). The experimental results indicate that the combustion reactivity of chars decreases with increasing graphitization degree. And an obvious liner relationship between  $f_a$  and  $T_{\max}/E$  was found.

**Keywords** Char · Microstructure · Combustion reactivity · Kinetics · XRD

### 12.1 Introduction

Coal combustion generally includes three steps: (i) pyrolysis or devolatilization to release volatiles; (ii) combustion of volatile; (iii) combustion of char particles. Compared with the rapid devolatilization process, the combustion processes of char is much slower. Therefore, char combustion is the rate-controlling step of the combustion process of coal (Miura et al. 1989). After heat treatment, the combustion reactivity of char decreases. With the increase of heat treatment temperature and time, this phenomenon is becoming more obvious (Zhang et al. 2004). The microstructure of coal also changes in the process of char formation, including the loss of functional groups and the carbon microstructure changing to graphite. The change of

---

J. Li · L. Feng · Y. Huang · Y. Zhang · L. Junfu · M. Zhang (✉)  
Key Laboratory for Thermal Science and Power Engineering of Ministry of Education,  
Department of Energy and Power Engineering, Tsinghua University, Beijing, China  
e-mail: zhangman@mail.tsinghua.edu.cn

© Tsinghua University Press. 2022  
J. Lyu and S. Li (eds.), *Clean Coal and Sustainable Energy*,  
Environmental Science and Engineering,  
[https://doi.org/10.1007/978-981-16-1657-0\\_12](https://doi.org/10.1007/978-981-16-1657-0_12)

char microstructure after heat treatment is recognized as the major reason for the decrease of char combustion reactivity (Lu et al. 2002). Therefore, many studies have reported the relation between combustion reactivity and microstructure.

So far, many techniques have been employed to measure the microstructure of char, such as X-ray diffraction, transmission electron microscopy, and Raman spectroscopy (Oluwadayo 2010). X-ray diffraction does not cause destruction to the sample, so it was widely used to obtain the structural information, considering the crystalline carbon and amorphous carbon for carbon structure. Quantitative analysis of X-ray diffraction yields several parameters, including crystallite size ( $L_a$ ,  $L_c$ ,  $d_{002}$ ,  $g$ ) and aromaticity ( $f_a$ ) (Lu et al. 2001).

Lu et al. (2002) used low volatile bituminous coal to prepare char samples. They found that even at very low temperature, char structure was more ordered during combustion. The amorphous concentration, which can reflect char structure, was decreased, while the aromaticity and average crystallite size was increased. As a result, char becomes less reactive. They also defined an index of disorder,  $IOD$ , to quantitatively describe char structure.

Zhu and Sheng (2010) used a non-isothermal TGA method to measure char combustion reactivity, and correlated the results with the first-order Raman parameters. A lignite was pyrolyzed from 773 to 1673 K. A good linear correlations were found between combustion reactivity indexes and the band area ratios of  $I_{D1}/I_G$  and  $I_G/I_{ALL}$ .

Similar work had also been carried out by Everson et al. (2013). They found that the reactivity was depended on aromaticity. The intrinsic activity decreased significantly and activation energy increased with the increase of aromaticity.

However, in the related reported studies, the coal types used in the experiments were limited. Therefore, this work was addressed to the evolution of the microstructure of char under heat treatment and its influence on combustion reactivity for more different char samples. 12 samples, including anthracite, bituminous, lean coal and lignite, were used for char preparation at 900 °C. The combustion reactivity of char was measured with the thermogravimetric analyzer based on a non-isothermal method. The microstructure was measured by X-ray diffraction. The relationship between the char combustion reactivity and microstructure were discussed.

## 12.2 Experimental

### 12.2.1 Coal Samples and Preparation of Char

The experiment using chars from different coals. There are 12 kinds of coal coming different regions, including anthracite, bituminous, lean coal and lignite. And the particle size was 75–100  $\mu\text{m}$ . The properties of the samples are presented in Tables 12.1 and 12.2.

**Table 12.1** Proximate analysis of coal

Sample ID		Ma	Va	Aa	Fca	Vd	Ad	Vdaf
Anthracite	XR	3.66	4.85	17.45	74.04	5.03	18.11	6.15
	YQ	2.56	8.34	10.02	79.08	8.56	10.28	9.54
	HN	0.81	5.65	16.05	77.49	5.70	16.18	6.80
Lean coal	QB	1.52	10.09	24.41	63.98	10.25	24.79	13.62
	HD	2.70	12.28	25.89	59.13	12.62	26.61	17.20
Bituminous	QJY	1.63	19.28	35.72	43.37	19.60	36.31	30.77
	ZY	4.43	25.65	33.23	36.69	26.84	34.77	41.15
	PS	5.00	26.24	32.91	35.85	27.62	34.64	42.26
Lignite	XL	27.45	28.75	15.71	28.09	39.63	21.65	50.58
	HLH	23.88	27.20	26.80	22.12	35.73	35.21	55.15
	CY	19.96	25.26	26.13	28.65	31.56	32.65	46.86
	SZ	16.62	41.34	8.84	33.20	49.58	10.60	55.46

**Table 12.2** Ultimate analysis of coal

Sample ID		C%	H%	O%	N%	S%
Anthracite	XR	72.74	2.50	0.82	0.26	1.66
	YQ	79.83	3.09	2.04	0.27	0.78
	HN	78.30	0.16	1.68	0.11	2.09
Lean coal	QB	68.88	3.06	0.01	0.46	0.51
	HD	59.90	3.42	4.56	0.44	0.61
Bituminous	QJY	51.16	3.19	5.98	1.35	0.98
	ZY	43.86	3.33	13.43	1.00	0.71
	PS	47.72	3.54	7.91	1.15	1.76
Lignite	XL	33.42	2.65	22.31	0.48	0.86
	HLH	35.43	2.53	9.60	0.74	0.45
	CY	11.18	0.80	38.15	0.13	0.34
	SZ	49.08	4.06	19.35	1.01	1.06

The char samples were prepared in the muffle furnace at ambient atmosphere in 900 °C. Before preparation, the sample was placed in a dry box and dried at 105 °C for two hours to remove moisture.

### 12.2.2 Char Characterization

In order to test the properties of char, proximate analysis has been carried out. And the result is showed in Table 12.3. All samples should be stored in dry condition.

**Table 12.3** Proximate analysis of char

Sample ID		Ma	Va	Aa	FCa
Anthracite	XR	0.81	3.98	16.24	78.97
	YQ	0.72	5.80	8.95	84.53
	HN	0.01	4.48	18.13	77.38
Lean coal	QB	0.61	6.03	23.60	69.76
	HD	0.43	5.46	29.07	65.03
Bituminous	QJY	0.35	3.27	43.55	52.83
	ZY	1.95	4.76	42.61	50.68
	PS	0.58	3.52	43.25	52.65
Lignite	XL	0.82	6.50	19.21	73.48
	HLH	0.78	5.07	50.90	43.26
	CY	0.77	5.68	45.09	48.46
	SZ	0.87	5.22	15.12	78.79

### 12.2.3 X-Ray Diffraction Analysis

D8-Discover X-ray diffractometer was used to record X-ray intensities scattered from char samples. Cu K $\alpha$  radiation (40 kV, 40 mA) was used as the X-ray source. Samples were scanned over the angular  $2\theta$  range of  $5^\circ$  to  $80^\circ$ , and in a step-scan mode with a step size of  $0.02^\circ$ . Two peaks were expected over the examined  $2\theta$  range, the (002) peak and (10) peak. The position of the peak in the low angle corresponds to the (002) peak of graphite, which is attributed to the stacking of the graphitic basal plans of char crystallites. The peak in the high angle called (10) peak, which is attributed to hexagonal ring structure in char crystallites. Theoretically, the (002) peak symmetric, but the pattern shows obvious asymmetry. This is due to the existence of  $\gamma$  band on the left of (002) peak. And it is associated with packing of saturated structure such as aliphatic side chains (Watanable et al. 2002).

We can obtain four structural parameters based on XRD, viz. crystallite height ( $L_c$ ), crystallite diameter ( $L_a$ ), interlayer spacing ( $d_{002}$ ) and aromaticity ( $f_a$ ). They can be calculated by Eqs. (12.1)–(12.4).

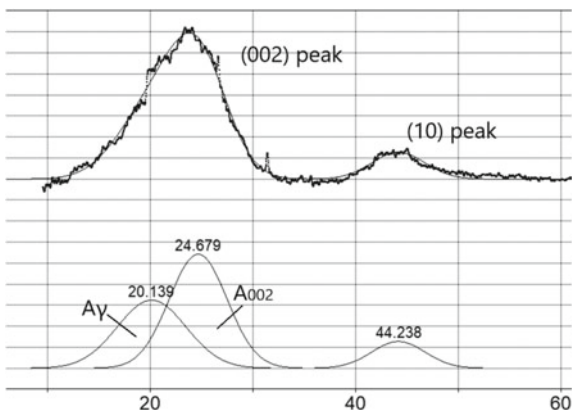
$$d_{002} = \frac{\lambda}{2 \sin \theta_{002}} \quad (12.1)$$

$$L_c = \frac{0.89\lambda}{\beta_{002} \cos \theta_{002}} \quad (12.2)$$

$$L_a = \frac{1.84\lambda}{\beta_{10} \cos \theta_{10}} \quad (12.3)$$

$$f_a = \frac{A_{002}}{A_{002} + A_\gamma} \times 100\% \quad (12.4)$$

**Fig. 12.1** X-ray diffraction pattern



where  $\lambda$  is the wavelength of the incident X-rays ( $\text{\AA}$ ). For copper  $K\alpha$  radiation, the  $\lambda$  value is  $1.5406 \text{ \AA}$ . The  $\theta$  is the peak position,  $\beta$  is the full width of the peak at half maximum intensity. And  $A$  is the area under the corresponding peak respectively.

As a function of heat treated conversion process, these parameters would be gradually evolved with the coal oxidation process. With the structure of char tending to be ordered,  $L_c$ ,  $L_a$  and  $f_a$  will increase with decreasing  $d_{002}$  (Fig. 12.1).

### 12.2.4 Char Combustion Reactivity Measurement

Char combustion reactivity was measured by a thermogravimetric analyzer (Mettler-Toledo TGA/DSC1/1600HT) in non-isothermal method. The reaction was performed in the air atmosphere with 21%  $O_2$ . About 10 mg of char samples was placed in the TGA pan, and heat from room temperature to  $1000 \text{ }^\circ\text{C}$  at a heating rate of  $15 \text{ K/min}$ . And then the chars were cooled to the programmed temperature. The gas flow rate is  $100 \text{ ml/min}$ . And the temperature and weight of sample can be recorded (Nie et al. 2001).

The conversion of the char at any time can be calculated by Eq. (12.5).

$$X = \frac{m_0 - m}{m_0 - m_{ash}} \times 100\% \tag{12.5}$$

where  $m_0$  is the initial weight of sample and  $m_{ash}$  is the weight at the end of the reaction.

Define  $R$  as the combustion rate:

$$R = \left( \frac{dX}{dt} \right)_{\max} \tag{12.6}$$

In addition, according to the non-isothermal method, we can obtain the initial temperature of combustion reaction ( $T_i$ ), the temperature corresponding to the maximum reaction rate ( $T_{\max}$ ) and the temperature at the end of reaction. We can also define the temperature corresponding to 20% conversion as characteristic temperature.

Kinetic parameters of combustion reaction can be obtained from Arrhenius equation

$$\frac{dX}{dt} = A \exp\left(-\frac{E}{RT}\right)(1-X)^n \quad (12.7)$$

where  $A$  is pre-exponential factor,  $E$  is activation energy,  $R$  is universal gas constant and  $n$  is reaction order. For non-isothermal method, a constant heating rate  $\beta$  is introduced into the equation. By transforming the equation, can get the following equation (Xie 2002)

$$\begin{aligned} \ln\left[\frac{1 - \ln(1-X)^{1-n}}{T^2(1-n)}\right] &= \ln\left(\frac{AR}{\beta E}\right) - \frac{E}{RT}n \neq 1 \\ \ln\left[-\frac{\ln(1-X)}{T^2}\right] &= \ln\left(\frac{AR}{\beta E}\right) - \frac{E}{RT}n = 1 \end{aligned} \quad (12.8)$$

Therefore, the activation energy of the reaction can be used to characterize the combustion reactivity of char, and it was derived by fitting the Arrhenius plot with the reaction rate in the conversion range of 20–80% for each sample. The conversion of 20% was chosen as the low limit to avoid the measurement uncertainty at very low conversion.

## 12.3 Results and Discussion

### 12.3.1 X-Ray Diffraction Carbon Crystallite Analyses

The XRD diffraction pattern of char is shown in the Fig. 12.2. The curves show the representative samples selected from each kind of coal. The 002 peak is sharper and narrower with the increase of coal rank (Li 2013). This is because of a more compact, more ordered and more orientated structure.

The aromaticity ( $f_a$ ), inter layer spacing ( $d_{002}$ ), crystallite diameter ( $L_a$ ) and crystallite height ( $L_c$ ) are shown in Table 12.3. The small spikes on the diffractograms are peaks of traces of minerals still remaining in the samples (Table 12.4).

**Fig. 12.2** Diffractograms of different chars

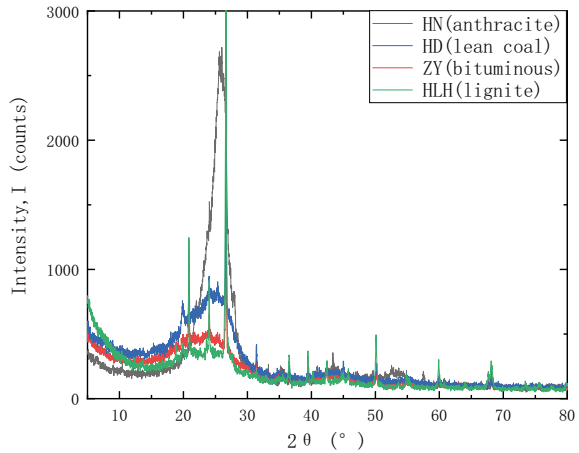


**Table 12.4** Carbon crystallite properties of char used for combustion experiments

Sample ID		Lc/Å	La/Å	fa/%	d <sub>002</sub> /Å
Anthracite	XR	15.26	40.87	71.31	1.83
	YQ	12.54	35.79	75.35	1.91
	HN	28.47	42.62	76.84	1.77
Lean coal	QB	15.95	31.61	66.49	1.83
	HD	14.27	36.45	67.78	1.82
Bituminous	QJY	15.58	31.34	71.70	1.80
	ZY	12.83	26.48	57.60	1.84
	PS	11.13	31.09	71.37	1.89
Lignite	XL	11.84	35.97	49.74	1.91
	HLH	11.32	38.79	59.91	1.90
	CY	13.90	37.14	55.12	1.92
	SZ	10.34	40.73	62.37	1.93

### 12.3.2 Char Combustion Reactivity

The combustion reactivity of char is affected by many factors, including the process of getting char, the nature of the original sample and so on. Several representative thermogravimetric curves of char are listed in Fig. 12.3. The parameters of char combustion reactivity are listed in Table 12.5.

The combustion reactivity of chars made from different kinds of coal under the same conditions is quite different. The initial temperature of combustion reaction ( $T_i$ ) is at about 400 °C, and the temperature corresponding to the maximum reaction rate ( $T_{max}$ ) is at about 600 °C. Actually, it was observed that all chars were completely

**Fig. 12.3** Char conversion is plotted as a function of the temperature

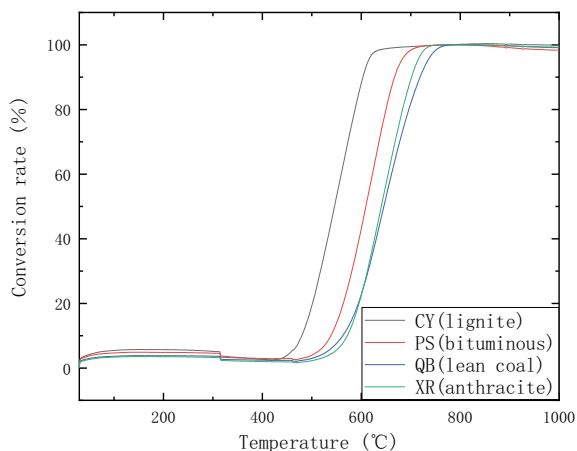


**Table 12.5** The parameters of char combustion reactivity

Sample ID		Tmax (°C)	Ti (°C)	Tf (°C)	T20 (°C)	R	E (J/mol)
Anthracite	XR	638.00	468.31	777.14	600.61	0.19	2.44E+05
	YQ	652.90	468.17	790.71	609.63	0.16	2.48E+05
	HN	720.86	467.83	830.54	610.36	0.14	2.48E+05
Lean coal	QB	638.89	468.16	804.85	598.87	0.17	2.45E+05
	HD	638.24	468.18	829.34	605.65	0.17	2.47E+05
Bituminous	QJY	634.11	468.28	791.68	600.56	0.18	2.44E+05
	ZY	557.06	418.42	723.64	512.05	0.17	2.21E+05
	PS	617.39	468.00	752.41	568.68	0.19	2.35E+05
Lignite	XL	537.29	334.94	710.87	480.89	0.15	2.13E+05
	HLH	536.60	357.63	757.75	487.09	0.21	2.14E+05
	CY	547.74	419.53	711.15	502.82	0.19	2.18E+05
	SZ	598.94	419.05	777.55	524.54	0.14	2.26E+05

burned before 850 °C. The burnout temperature of each char was lower than the corresponding treatment temperature.

### 12.3.3 Correlations Between Char Combustion Reactivity and X-Ray Diffraction

It is clear that the aromaticity, inter layer spacing ( $d_{002}$ ), crystallite diameter ( $L_a$ ) and crystallite height ( $L_c$ ) are interrelated. So that any of these parameters can be chosen for correlating XRD properties with char combustion reactivity. And an obvious liner



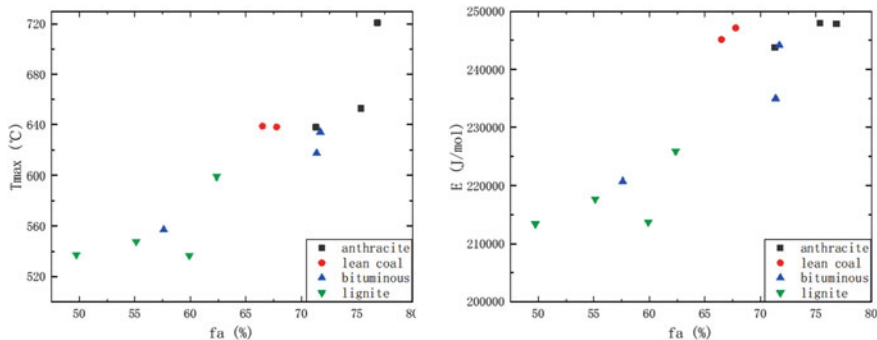


Fig. 12.4 Effect of aromaticity on char combustion reactivity

relationship between  $f_a$  and  $T_{max}/E$  exists and is presented in Fig. 12.4. The increase of  $T_{max}$  and  $E$  indicates that the reactivity of char decreases.

Figure 12.4 shows that  $T_{max}$  and  $E$  increase with the increasing aromaticity. Aromaticity is the fraction of aromatic carbon atoms within the char crystalline structure. The aromaticity in certain cases was as high as 0.75 has a very orderly structure. Therefore, the increase of aromaticity leads to more carbon microcrystals with ordered structure and orientation, which tend to graphite structure and with decreasing edge defects. This is consistent with previous studies.

Figure 12.5 shows that the effect of layer spacing ( $d_{002}$ ) on char combustion reactivity. The decrease of  $d_{002}$  indicates the ordering of char structure. Figure 12.5 shows that with the decrease of  $d_{002}$ ,  $T_{max}$  and  $E$  increase.

Figure 12.6 shows the effect of  $L_c$  and  $L_a$  on char combustion reactivity. Theoretically, with the increase of  $L_c$  and  $L_a$ , the combustion reactivity of char decreases, and correspondingly,  $T_{max}$  and  $E$  increase. But from the experimental results, the effect of  $L_c$  and  $L_a$  is not very obvious. At the same time, the change of  $L_c$  and  $L_a$  in the heat treatment process is staged and very complicated (Zubkova 2005; Li 2018).

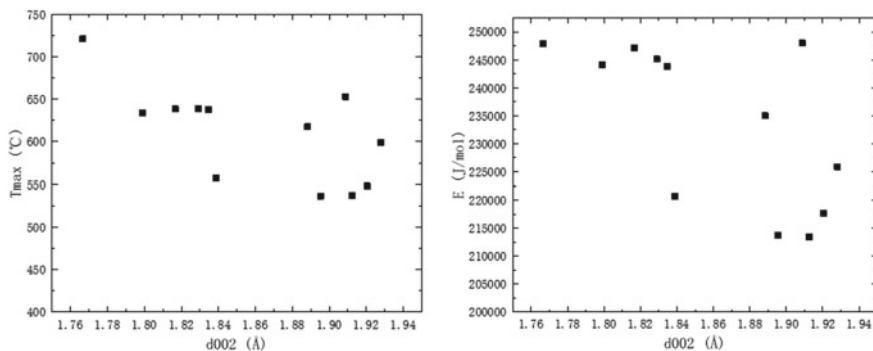
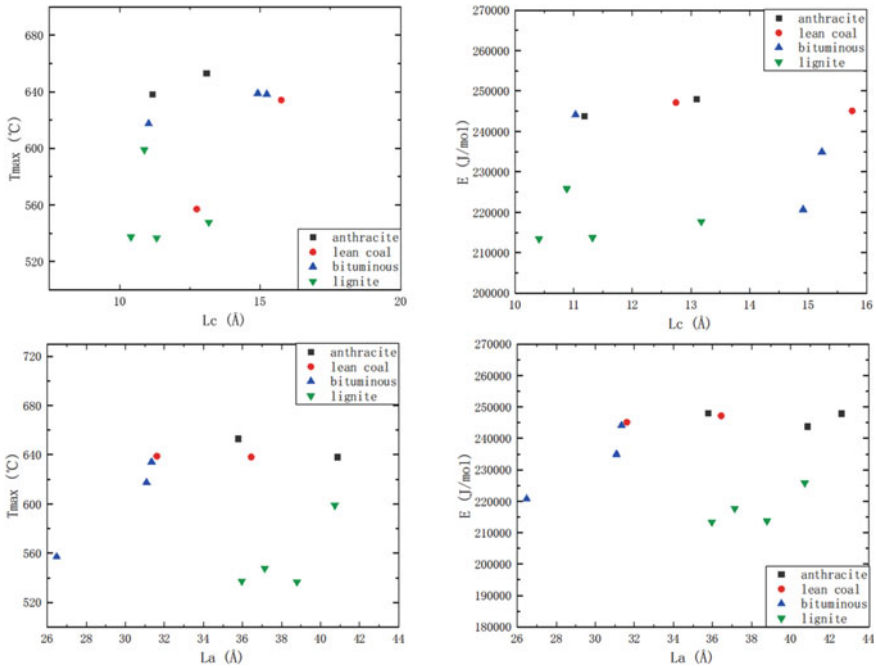


Fig. 12.5 Effect of layer spacing ( $d_{002}$ ) on char combustion reactivity



**Fig. 12.6** Effect of crystallite diameter ( $L_a$ ) and crystallite height ( $L_c$ ) on char combustion reactivity

## 12.4 Conclusions

In present work, the microstructure of chars and their combustion reactivity had been studied using thermogravimetric analyzer (TGA) and X-ray diffraction (XRD) analyzer, respectively. The correlations between structural parameters and combustion reactivity had been analyzed in detail. The key points of the present research are summarized below:

- (1) After heat treatment, the structure of chars tend to be ordered and the combustion reactivity of chars decrease. For all kinds of coal, combustion reactivity of chars decreases with increasing graphitization degree.
- (2) A strong liner relationship between  $f_a$  and  $T_{max}/E$  exists. The ordering of char structure is considered to be the main reason for the reduction of char combustion reactivity.

**Acknowledgements** This work was supported by the Key Project of Natural Science Foundation of China (No. 29936090) and the Special Funds for Major State Basic Research projects (G1999022102).

## References

- Everson RC, Okolo GN, Neomagus HW, Dos Santos JM (2013) X-ray diffraction parameters and reaction rate modeling for gasification and combustion of chars derived from inertinite-rich coals. *Fuel* 109:148–156
- Li Q (2018) Investigation on the structure evolution of pre and post explosion of coal dust using X-ray diffraction. *Int J Heat Mass Transf* 120:1162–1172
- Li M et al (2013) Aggregate structure evolution of low-rank coals during pyrolysis by in-situ X-ray diffraction. *Int J Coal Geol* 116–117:262–269
- Lu L, Sahajwalla V, Kong C, Harris D (2001) Quantitative X-ray diffraction analysis and its application to various coals. *Carbon* 39(12):1821–1833
- Lu L, Kong C, Sahajwalla V, Harris D (2002) Char structural ordering during pyrolysis and combustion and its influence on char reactivity. *Fuel* 81:1215–1225
- Miura K, Hashimoto K, Silveston PL (1989) Factors affecting the reactivity chars during gasification, representing reactivity. *Fuel* 68:1461–1475
- Nie QH, Sun SZ, Li ZQ, Zhang XJ, Wu SH, Qin YK (2001) Thermogravimetric analysis on the combustion characteristics of brown coal blends. *J Combust Sci Technol* 7:72–76
- Oluwadayo O (2010) Sonibare: structural characterization of Nigerian coals by X-ray diffraction, Raman and FTIR Spectroscopy. *Energy* 35:5347–5353
- Watanabe I, Sakanishi K, Mochida I (2002) Changes in coal aggregate structure by heat treatment and their coal rank dependency. *Energy & Fuels* 16:18–22
- Xie KC (2002) Coal structure and its reactivity. Science Press, Beijing, pp 221–222
- Zhang S, Lyu J et al (2004) Effect of heat treatment on the reactivity and microstructure of coal-char. *J Fuel Chem Technol* 32(6):673–678
- Zhu X, Sheng C (2010) Evolution of the char structure of lignite under heat treatment and its influences on combustion reactivity. *Energy Fuels* 24:152–159
- Zubkova VV (2005) Some aspects of structural transformation taking place in organic mass of Ukrainian coals during heating. Part 1. Study of structural transformations when heating coals of different caking capacity. *Fuel* 84:741–754